Supplementary Figures and Tables

Additional Time Series Plots NO3, EC and other

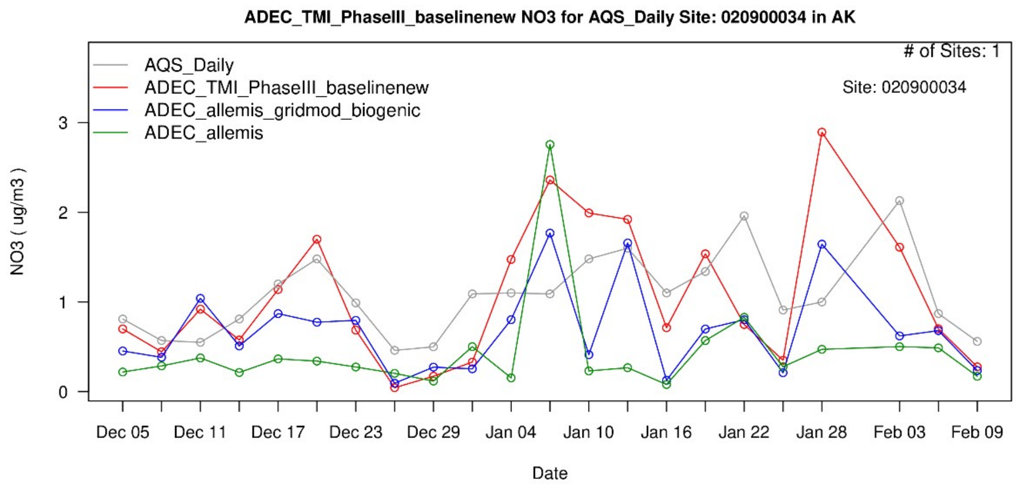

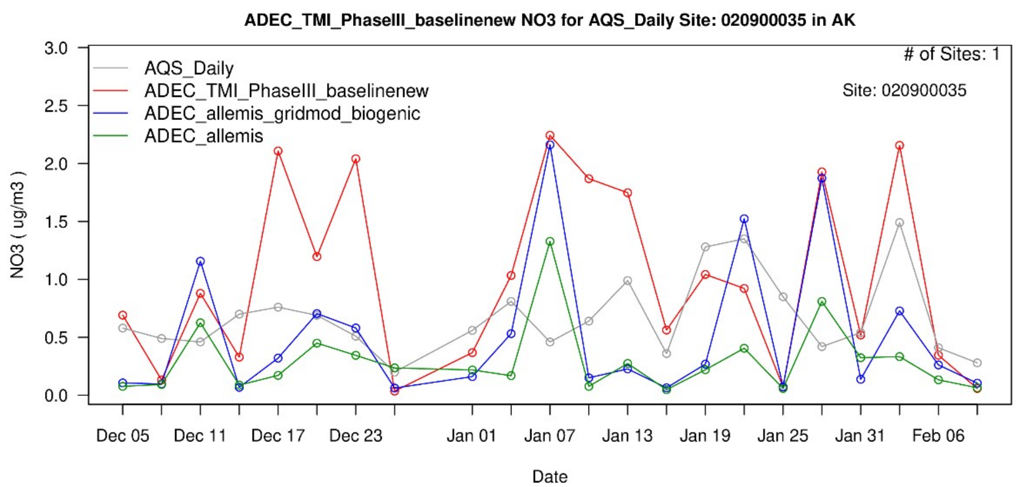

S 1: Timeseries of NO3 at NCore (020900034) and Hurst Road (020900035) monitors for the modeling period

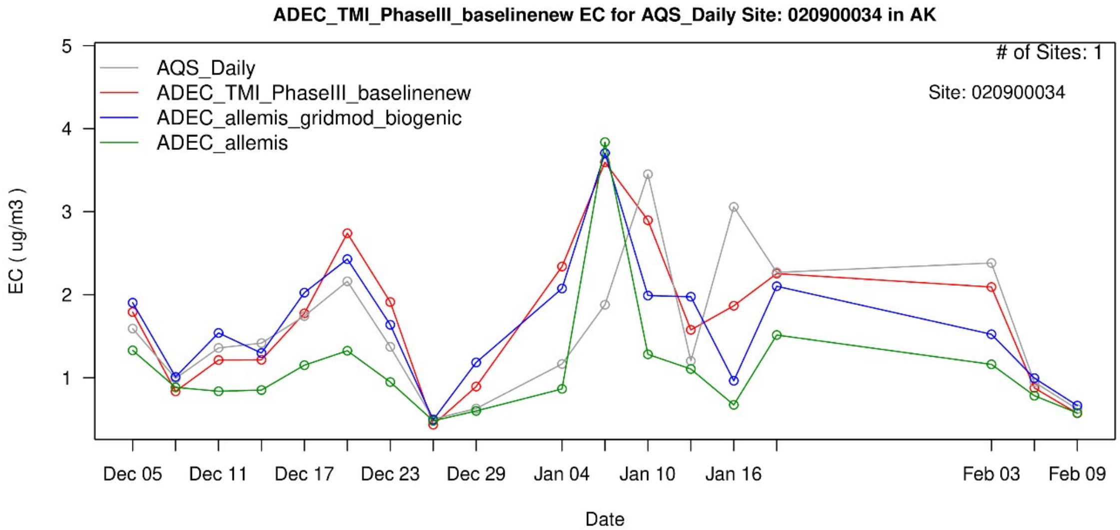

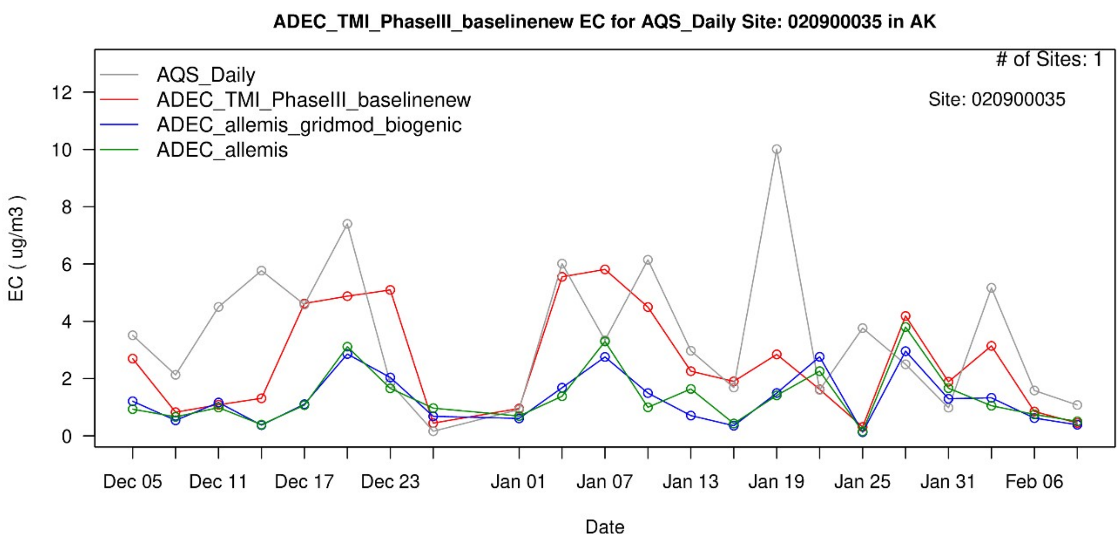

S 2: Timeseries of EC at NCore (020900034) and Hurst Road (020900035) monitors for the modeling period

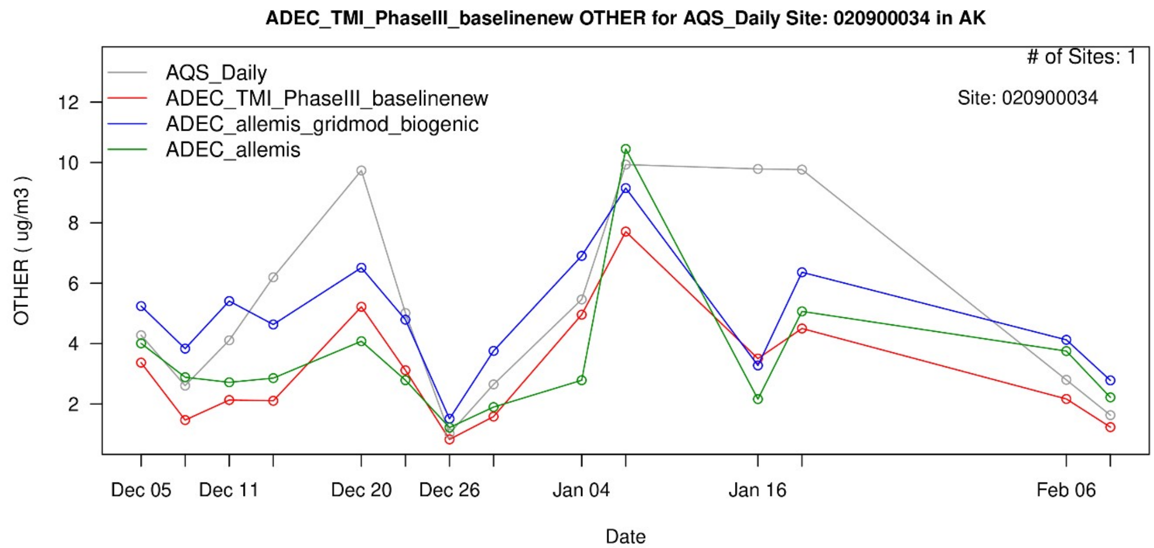

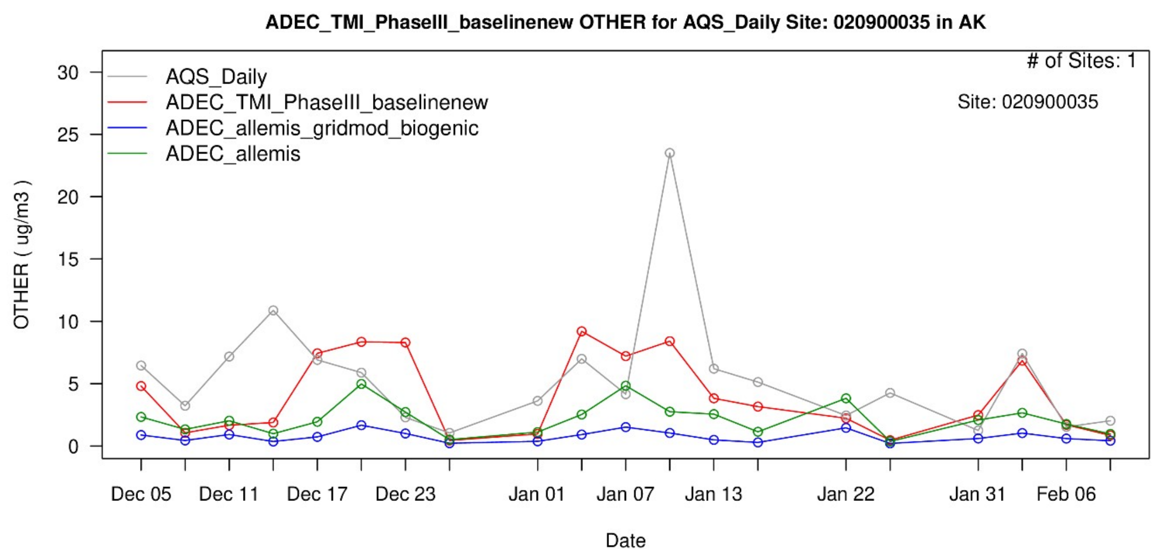

S 3: Timeseries of OTHER at NCore (020900034) and Hurst Road (020900035) monitors for the modeling period

S 4: Statistics of speciated PM and total PM2.5 for the modeling episode at Hurst Road monitor

Species	Number of Observations	Mean Obs (µg/m³)	Mean Model (µg/m³)	Mean Bias	Mean Error	Normalized Mean Bias (NMB, %)	Normalized Mean Error (NME, %)	Fractional Bias (FB, %)	Fractional Error (FE, %)	Root Mean Square Error (RMSE)	Correlation
NO3	22	0.67	1.01	0.60	0.34	50.2	88.5	5.5	73.3	0.79	0.33
SO4	22	2.26	2.52	1.10	0.26	11.5	48.8	4.9	44.0	1.68	0.50
NH4	22	0.80	1.12	0.61	0.33	41.1	76.5	37.9	66.0	0.86	0.43
EC	22	3.53	2.60	1.74	-0.93	-26.3	49.3	-25.9	59.8	2.45	0.45
OC	22	14.47	13.58	6.42	-0.89	-6.2	44.4	-8.9	57.8	9.24	0.64
PM_TOT	21	25.08	24.96	11.06	-0.12	-0.5	44.1	-9.3	50.1	16.11	0.61

S 5: Statistics of speciated PM and total PM2.5 for the modeling episode at NCore monitor

Species	Number of Observations	Mean Obs (µg/m³)	Mean Model (µg/m³)	Mean Bias	Mean Error	Normalized Mean Bias (NMB, %)	Normalized Mean Error (NME, %)	Fractional Bias (FB, %)	Fractional Error (FE, %)	Root Mean Square Error (RMSE)	Correlation
NO3	22	1.07	1.06	0.48	-0.01	-1.3	45.0	-22.6	52.2	0.65	0.51
SO4	22	3.41	3.29	1.21	-0.12	-3.4	35.4	-2.1	32.3	1.80	0.69
NH4	22	1.31	1.35	0.56	0.05	3.4	43.0	11.2	40.8	0.85	0.66
EC	18	1.60	1.72	0.42	0.12	7.5	26.5	6.0	23.1	0.63	0.71
OC	18	3.54	7.31	3.84	3.77	106.6	108.5	59.3	61.9	5.06	0.82
PM_TOT	18	15.31	18.16	5.68	2.85	18.6	37.1	9.7	27.8	8.52	0.72

S6 Emission Plots for each sector Aircraft, Area, Non-Road, On-Road, Point, Space-Heat and pollutant (PM2.5, NOx, SO2, VOC) for the control year 2027

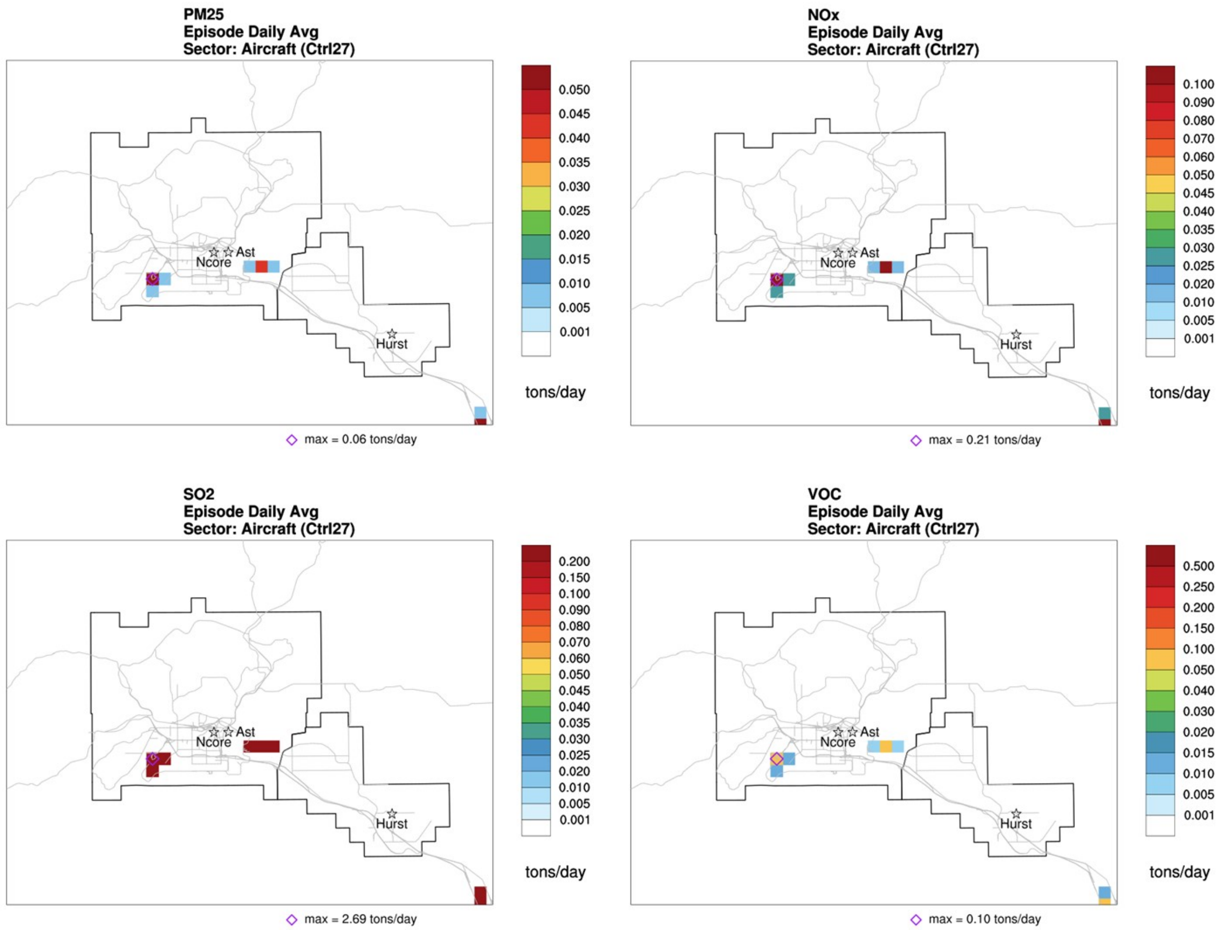

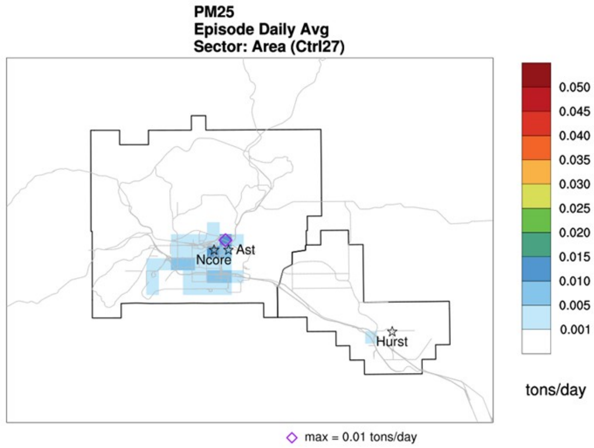
PM25
Episode Daily Avg
Sector: Area (Ctrl27)
0.050
0.045
0.040
0.035
0.030
0.025
0.020
0.015
0.010
0.005
0.001
tons/day
Ast
Ncore
Hurst
max = 0.01 tons/day

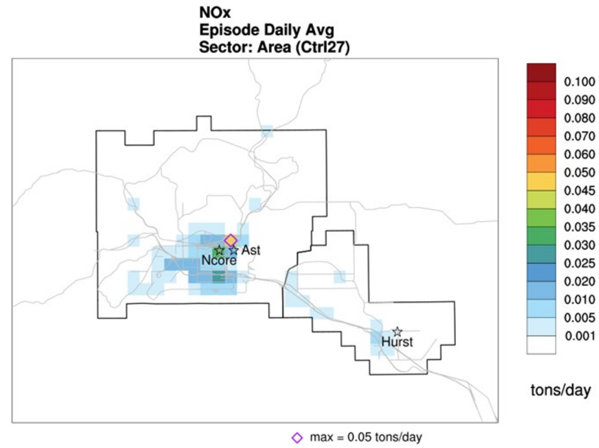
NOx
Episode Daily Avg
Sector: Area (Ctrl27)
0.100
0.090
0.080
0.070
0.060
0.050
0.045
0.040
0.035
0.030
0.025
0.020
0.010
0.005
0.001
tons/day
Ast
Ncore
Hurst
max = 0.05 tons/day

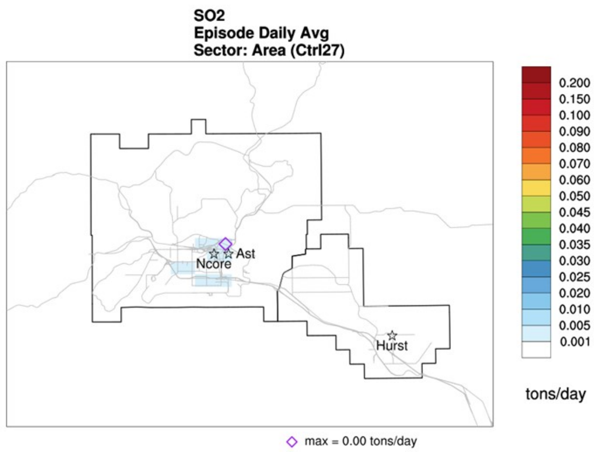
SO2
Episode Daily Avg
Sector: Area (Ctrl27)
0.200
0.150
0.100
0.090
0.080
0.070
0.060
0.050
0.045
0.040
0.035
0.030
0.025
0.020
0.010
0.005
0.001
tons/day
Ast
Ncore
Hurst
max = 0.00 tons/day

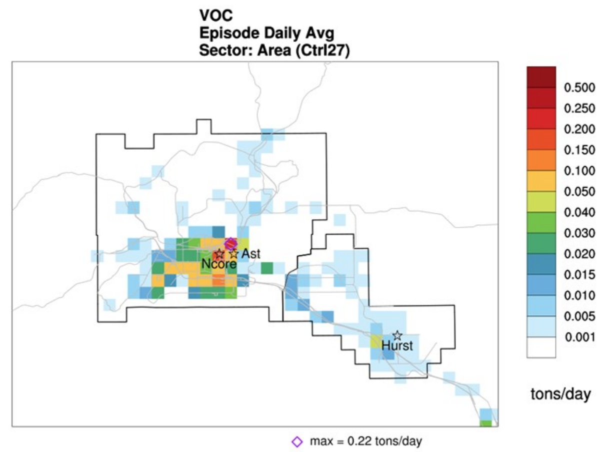
VOC
Episode Daily Avg
Sector: Area (Ctrl27)
0.500
0.250
0.200
0.150
0.100
0.050
0.040
0.030
0.020
0.015
0.010
0.005
0.001
tons/day
Ast
Ncore
Hurst
max = 0.22 tons/day

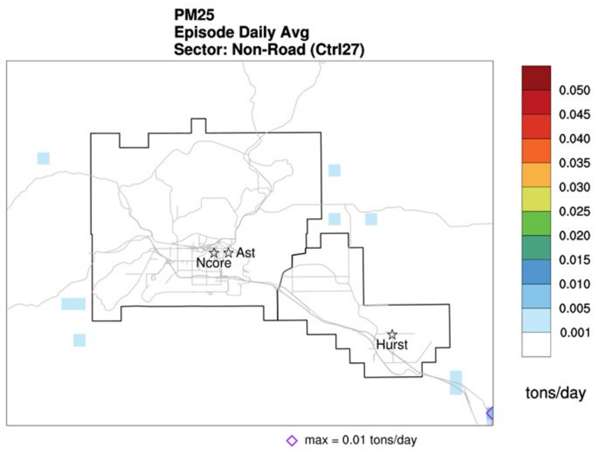
PM25
Episode Daily Avg
Sector: Non-Road (Ctrl27)
0.050
0.045
0.040
0.035
0.030
0.025
0.020
0.015
0.010
0.005
0.001
tons/day
Ast
Ncore
Hurst
max = 0.01 tons/day

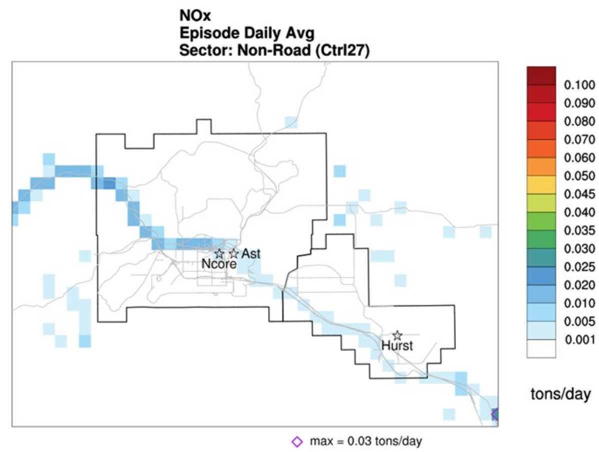
NOx
Episode Daily Avg
Sector: Non-Road (Ctrl27)
0.100
0.090
0.080
0.070
0.060
0.050
0.045
0.040
0.035
0.030
0.025
0.020
0.010
0.005
0.001
tons/day
Ast
Ncore
Hurst
max = 0.03 tons/day

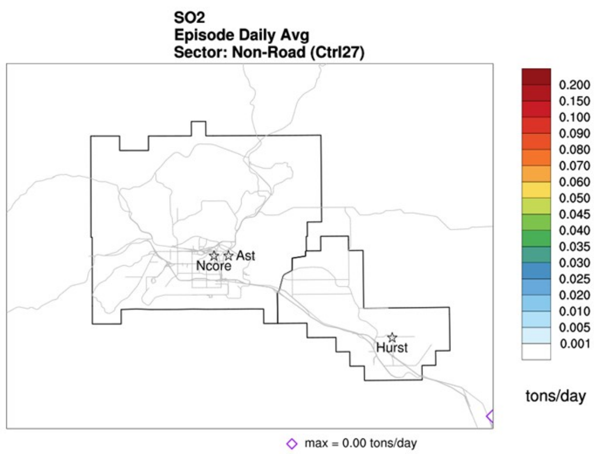
SO2
Episode Daily Avg
Sector: Non-Road (Ctrl27)
0.200
0.150
0.100
0.090
0.080
0.070
0.060
0.050
0.045
0.040
0.035
0.030
0.025
0.020
0.010
0.005
0.001
tons/day
Ast
Ncore
Hurst
max = 0.00 tons/day

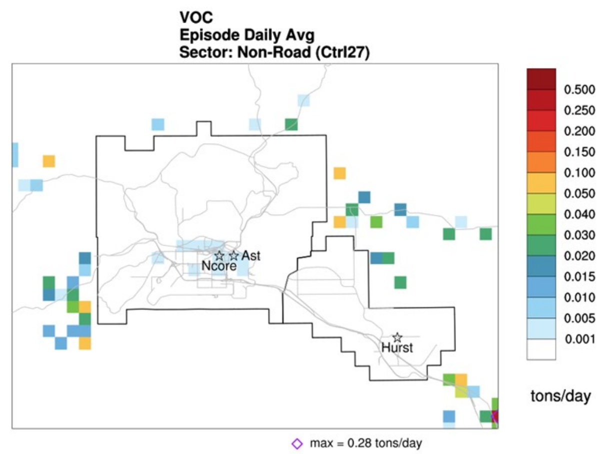
VOC
Episode Daily Avg
Sector: Non-Road (Ctrl27)
0.500
0.250
0.200
0.150
0.100
0.050
0.040
0.030
0.020
0.015
0.010
0.005
0.001
tons/day
Ast
Ncore
Hurst
max = 0.28 tons/day

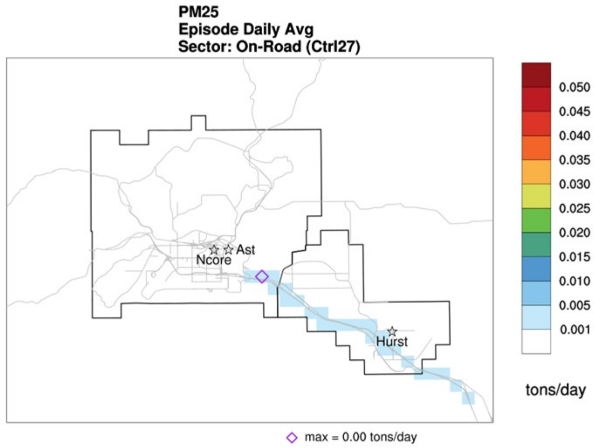
PM25
Episode Daily Avg
Sector: On-Road (Ctrl27)
Ast
Ncore
Hurst
0.050
0.045
0.040
0.035
0.030
0.025
0.020
0.015
0.010
0.005
0.001
tons/day
max = 0.00 tons/day

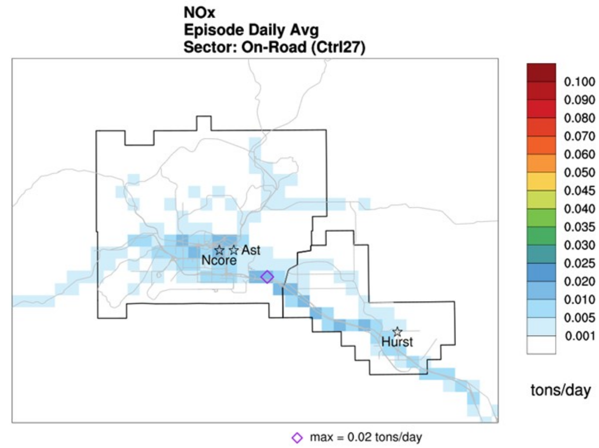
NOx
Episode Daily Avg
Sector: On-Road (Ctrl27)
Ast
Ncore
Hurst
0.100
0.090
0.080
0.070
0.060
0.050
0.045
0.040
0.035
0.030
0.025
0.020
0.010
0.005
0.001
tons/day
max = 0.02 tons/day

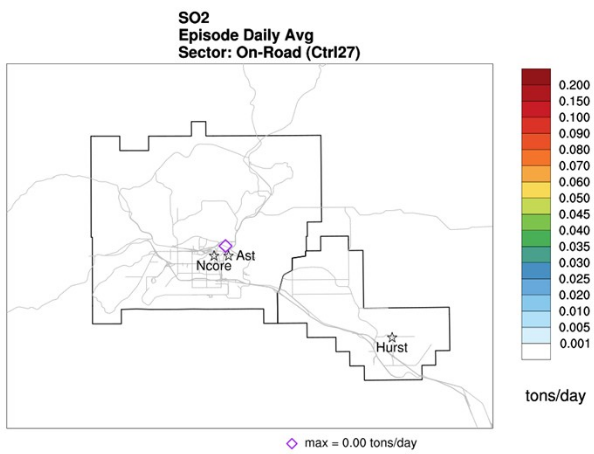
SO2
Episode Daily Avg
Sector: On-Road (Ctrl27)
Ast
Ncore
Hurst
0.200
0.150
0.100
0.090
0.080
0.070
0.060
0.050
0.045
0.040
0.035
0.030
0.025
0.020
0.010
0.005
0.001
tons/day
max = 0.00 tons/day

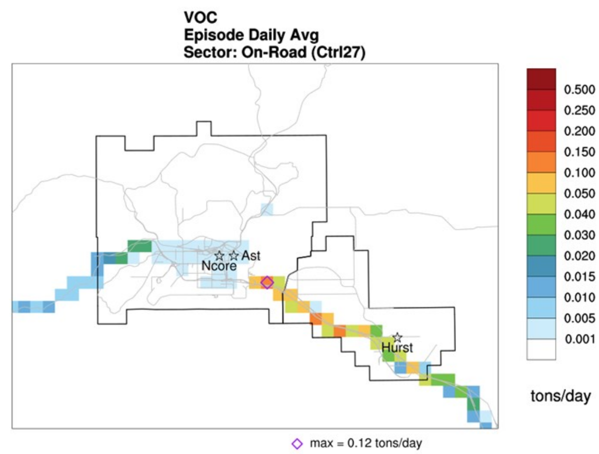
VOC
Episode Daily Avg
Sector: On-Road (Ctrl27)
Ast
Ncore
Hurst
0.500
0.250
0.200
0.150
0.100
0.050
0.040
0.030
0.020
0.015
0.010
0.005
0.001
tons/day
max = 0.12 tons/day

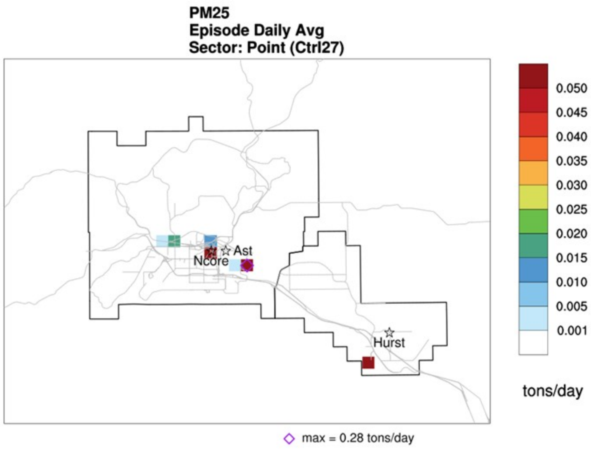
PM25
Episode Daily Avg
Sector: Point (Ctrl27)
Ast
Ncore
Hurst
0.050
0.045
0.040
0.035
0.030
0.025
0.020
0.015
0.010
0.005
0.001
tons/day
max = 0.28 tons/day

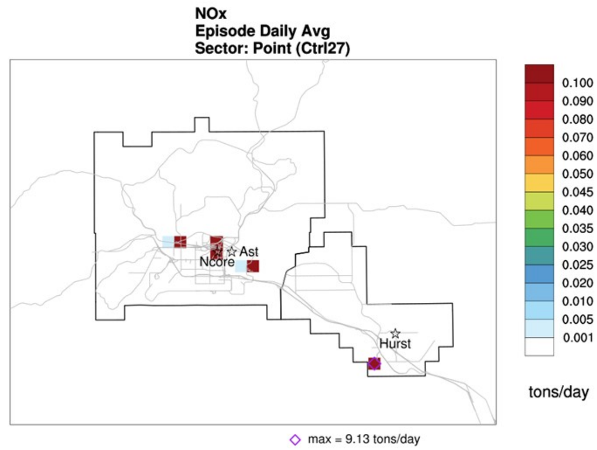
NOx
Episode Daily Avg
Sector: Point (Ctrl27)
Ast
Ncore
Hurst
0.100
0.090
0.080
0.070
0.060
0.050
0.045
0.040
0.035
0.030
0.025
0.020
0.010
0.005
0.001
tons/day
max = 9.13 tons/day

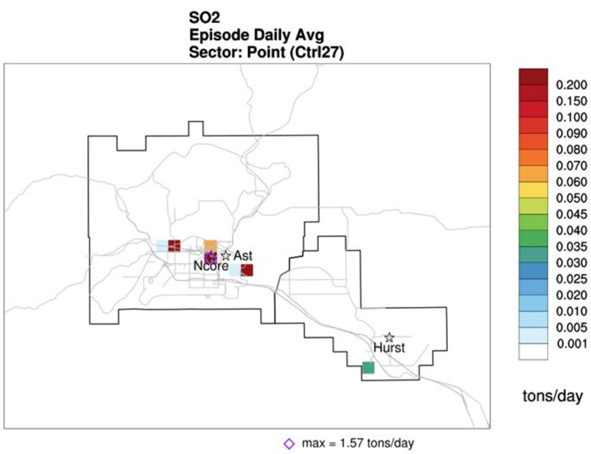
SO2
Episode Daily Avg
Sector: Point (Ctrl27)
Ast
Ncore
Hurst
0.200
0.150
0.100
0.090
0.080
0.070
0.060
0.050
0.045
0.040
0.035
0.030
0.025
0.020
0.010
0.005
0.001
tons/day
max = 1.57 tons/day

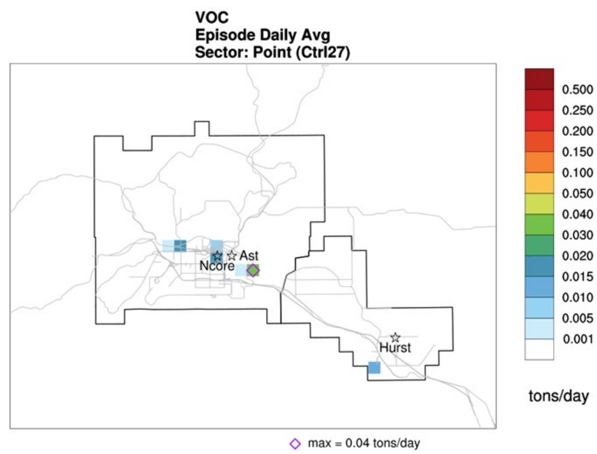
VOC
Episode Daily Avg
Sector: Point (Ctrl27)
Ast
Ncore
Hurst
0.500
0.250
0.200
0.150
0.100
0.050
0.040
0.030
0.020
0.015
0.010
0.005
0.001
tons/day
max = 0.04 tons/day

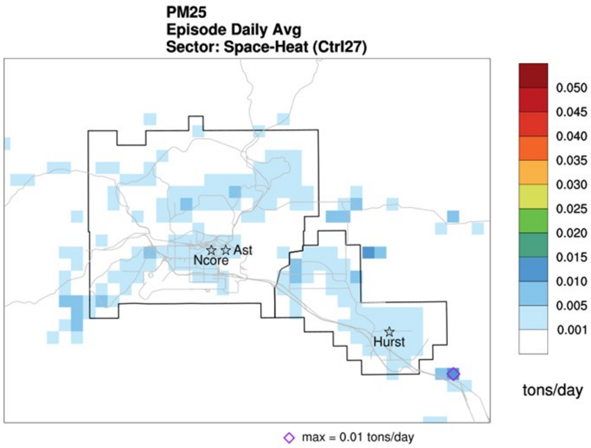
PM25
Episode Daily Avg
Sector: Space-Heat (Ctrl27)
Ast
Ncore
Hurst
0.050
0.045
0.040
0.035
0.030
0.025
0.020
0.015
0.010
0.005
0.001
tons/day
max = 0.01 tons/day

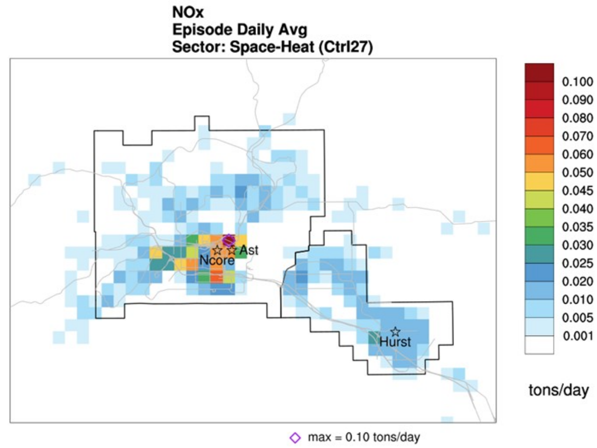
NOx
Episode Daily Avg
Sector: Space-Heat (Ctrl27)
Ast
Ncore
Hurst
0.100
0.090
0.080
0.070
0.060
0.050
0.045
0.040
0.035
0.030
0.025
0.020
0.010
0.005
0.001
tons/day
max = 0.10 tons/day

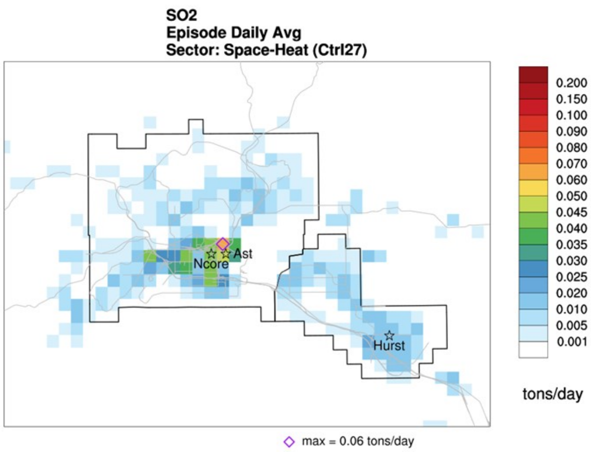
SO2
Episode Daily Avg
Sector: Space-Heat (Ctrl27)
Ast
Ncore
Hurst
0.200
0.150
0.100
0.090
0.080
0.070
0.060
0.050
0.045
0.040
0.035
0.030
0.025
0.020
0.010
0.005
0.001
tons/day
max = 0.06 tons/day

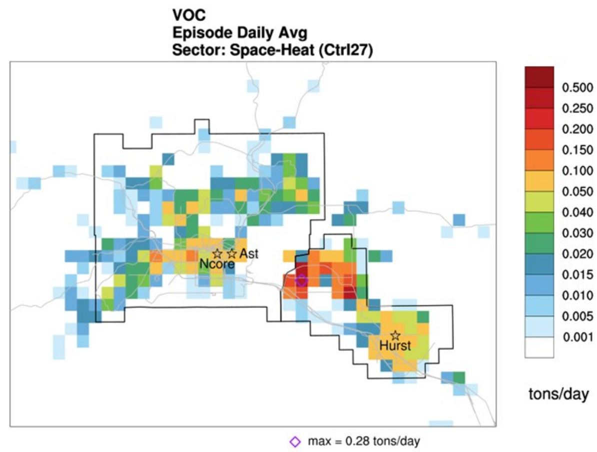
VOC
Episode Daily Avg
Sector: Space-Heat (Ctrl27)
Ast
Ncore
Hurst
0.500
0.250
0.200
0.150
0.100
0.050
0.040
0.030
0.020
0.015
0.010
0.005
0.001
tons/day
max = 0.28 tons/day

S 7 SO_2 Precursor Summary

			Episode Average			Max Daily Value	
CMAQ Sensitivity 100%		A Street	NCore	Hurst	A Street	NCore	Hurst
CMAQ - Absolute							
	SOx	-0.08703	-0.14015	-0.06109	-0.23067	-0.37986	-0.60623
CMAQ - Design Value							
	SOx	-0.21665	-0.14372	-0.21052			

The Emission Factors for space heating and for point sources are attached in excel spreadsheets:

EFs_SpaceHeating_RevSIP.xlsx

PointSource_EFs_By_EmissionUnit.xlsx

The SCC codes that were replaced with OMNI locally tested wood profiled are attached: in Speciations_SpaceHeating_OMNI.xlsx

From SMOKE, gspro_ptnonipm_cmaq_cb05_omni_100518.txt

The species specific RRFs and Future DV calculations are in the manual SMAT spreadsheet:

SMAT_091523.xls

Details on the updated to CMAQv5.3.3+

Updates were made to CMAQv5.3.3+ to add a representation of heterogeneous sulfur chemistry in aerosol water, including the formation and loss of hydroxymethanesulfonate (HMS). Aqueous aerosol sulfur reactions were parameterized with a reactive probability formulation (Cheng et al., 2016; Shao et al., 2019; Jacob, 2000) as follows:

$$\frac{dSO_4^{2-}}{dt} = k \times [SO_2\ or\ reactant], \quad (1)$$

$$k = \left(\frac{r}{D_g} + \frac{4}{v\gamma}\right)^{-1} A, \quad (2)$$

$$\gamma = \left(\frac{1}{\alpha} + \frac{v}{4H^* RT\sqrt{D_a k_{chem}}}\frac{1}{f_q}\right)^{-1}, \quad (3)$$

$$f_q = \left(coth(q) - \frac{l}{q}\right), \quad (4)$$

$$q = r\left(\frac{k_{chem}}{D_a}\right)^{0.5}, \quad (5)$$

where r = particle radius, D_g = gas-phase diffusivity of SO_2 or reactant, ν = mean molecular speed of SO_2 or reactant, A = aerosol surface area, γ = reactive uptake coefficient, α = accommodation coefficient of SO_2 or reactant, H^* = effective Henry's law coefficient of SO_2 or reactant, R = ideal gas constant, T = temperature (K), D_a = aqueous diffusion coefficient, k_{chem} =

(pseudo) first-order aqueous-phase reaction rate coefficient, and q = the diffuso-reactive parameter (Schwartz and Frieberg, 1981).

The uptake gas was determined by the limiting mass transfer rate, $J_{aq,lim}$:

$$J_{aq,lim} = min\{J_{SO2}, J_{RXT}\}\ , \tag{6}$$

where

$$J_x = k_{mt,x} H^*_x p_{x,\infty}\ , \tag{7}$$

$$k_{mt,x} = \left[\frac{r^2}{3D_g} + \frac{4r}{3\alpha v}\right]^{-1}\ , \tag{8}$$

where "x" = SO_2 or reactant (RXT) for a given reaction, $p_{x,\infty}$ = partial pressure of species x in the bulk gas phase, and ν = mean molecular speed of x. The aqueous concentration of the other (non-limiting) reactant is rolled into the pseudo-first order reaction rate coefficient, k_{chem} [s^{-1}]. For species originating in the gas phase, the aqueous concentration [M] is estimated with the effective Henry's law coefficient and partial pressure, [X] = $H^*_x\ p_{x,\infty}$. Concentrations [M] of species that primarily reside in the aerosol phase are estimated using the mass concentration of the species in air [μg m^{-3} air], molecular weight [g mol-1], and the accumulation mode volume concentration [$m^3\ m^{-3}$ air]. [H^+], inorganic aerosol liquid water content (ALW), and the phase distribution of semi-volatile inorganic species is provided by ISORROPIA II (Fountoukis and Nenes, 2007). Water associated with organics is estimated as described in Pye et al. (2017) with total aerosol liquid water content equal to the sum of inorganic and organic water.

Significant uncertainty lies in the S(IV) oxidation rates in aerosol water, where concentrations are orders of magnitude higher than the dilute (cloud-like) conditions under which many of the aqueous-phase oxidation rates were determined. The rates may be enhanced or inhibited with increasing ionic strength, and this is an active area of research (Liu et al., 2021). Here we applied ionic strength (enhancement and/or inhibition) factors (ISF) to adjust rate coefficients when shifting from a cloud- to aerosol-water environment. Ionic strength used to calculate aerosol water ISFs is estimated from the concentrations of the transported dissociating aerosol species but limited to the maximum ionic strength in the experiments investigating a particular ISF. As in Farrell et al. (2024), ISFs were used to adjust the rate coefficients for the oxidation of SO_2 by H_2O_2, O_3, and transition metal-catalyzed O_2 (TMI) as well as the effective Henry's law coefficients for SO_2 and H_2O_2. Also included is the ionic-strength dependent reaction rate for the reaction of S(IV) with NO_2 as described in Chen et al. (2019). In the cases where multiple oxidation rate expressions have been suggested in the literature (i.e., TMI and NO_2), the rates have been averaged with equal weighting. For more information on rate expressions, coefficients, and other parameters, please refer to Fahey et al. (in preparation) and Farrell et al. (2024).

Cloud/fog chemistry is modeled using CMAQ's KMT2 cloud option (Fahey et al., 2017; Fahey et al., submitted). This cloud module includes the formation and loss of HMS as well as inorganic S(IV) oxidation by H_2O_2, O_3, transition metal-catalyzed O_2, methyl hydroperoxide, peroxyacetic acid, peroxynitric acid, NO_2, OH and NO_3 radicals, and N(III). ISFs are not applied to chemical rates in cloud/fog water.

References:

Cheng, Y., Zheng, G., Wei, C., Mu, Q., Zheng, B., Wang, Z., Gao, M., Zhang, Q., He, K., Carmichael, G., Pöschl, U., and Su, H.: Reactive nitrogen chemistry in aerosol water as a source of sulfate during haze events in China, Sci. Adv., 2016.

Chen, T., Chu, B., Ge, Y., Zhang, S., Ma, Q., He, H., and Li, S.-M.: Enhancement of aqueous sulfate formation by the coexistence of NO2/NH3 under high ionic strengths in aerosol water. Environmental Pollution, 252, 236-244. doi:https://doi.org/10.1016/j.envpol.2019.05.119, 2019.

Fahey, K. M., Carlton, A. G., Pye, H. O. T., Baek, J., Hutzell, W. T., Stanier, C. O., Baker, K. R., Appel, K. W., Jaoui, M., and Offenberg, J. H., 2017. A framework for expanding aqueous chemistry in the Community Multiscale Air Quality (CMAQ) model version 5.1, Geosci. Model Dev., 10, 1587–1605, https://doi.org/10.5194/gmd-10-1587-2017.

Fahey, K.M., Gilliam, R.C., Pouliot, G., Huff, D., Murphy, B.N., Holder, A., Martin, J., Briggs, N., Farrell, S., Kotchenruther, R., Pye, H.O.T., and Sarwar, G.: Predicting PM2.5 in and around Fairbanks with the Community Multiscale Air Quality modeling system during the ALPACA winter air quality study, in preparation.

Fahey, K.M., Sareen, N., Carlton, A.G., and Hutzell, W.T. Updated in-cloud secondary aerosol production in the Northern Hemisphere predicted by the Community Multiscale Air Quality Modeling System version 5.3. Submitted.

Farrell, S. L., Pye, H. O. T., Gilliam, R., Pouliot, G., Huff, D., Sarwar, G., Vizuete, W., Briggs, N., and Fahey, K.: Predicted impacts of heterogeneous chemical pathways on particulate sulfur over Fairbanks, Alaska, the N. Hemisphere, and the Contiguous United States, EGUsphere [preprint], https://doi.org/10.5194/egusphere-2024-1550, 2024.

Fountoukis, C. and Nenes, A., 2007. ISORROPIA II: a computationally efficient thermodynamic equilibrium model for K+–Ca2+–Mg2+–NH4+–Na+–SO42—NO3—Cl—H2O aerosols, Atmos. Chem. Phys., 7, 4639–4659, https://doi.org/10.5194/acp-7-4639-2007.

Jacob, D.J.: Heterogeneous chemistry and tropospheric ozone, Atmospheric Environment, 34, 2131-2159, 2000.

Liu, T., Chan, A.W.H., and Abbatt, J.P.D.: Multiphase Oxidation of Sulfur Dioxide in Aerosol Particles:

Implications for Sulfate Formation in Polluted Environments, Environ. Sci. Technol., 55, 4227-4242, 2021.

Pye, H. O. T., Murphy, B. N., Xu, L., Ng, N. L., Carlton, A. G., Guo, H., Weber, R., Vasilakos, P., Appel, K. W.,

Budisulistiorini, S. H., Surratt, J. D., Nenes, A., Hu, W., Jimenez, J. L., Isaacman-VanWertz, G., Misztal, P. K., and

Goldstein, A. H.: On the implications of aerosol liquid water and phase separation for organic aerosol mass,

Atmos.Chem. Phys., 17, 343–369, https://doi.org/10.5194/acp-17-343-2017, 2017.

Schwartz, S. E. and Freiberg, J. E.: Mass-transport limitation to the rate of reaction of gases in liquid droplets: application to oxidation of SO_2 in aqueous solutions, Atmos. Environ., 15, 1129–1144, doi:10.1016/0004-6981(81)90303-6, 1981.

Shao, J., Chen, Q., Wang, Y., Lu, X., He, P., Sun, Y., Shah, V., Martin, R. V., Philip, S., Song, S., Zhao, Y., Xie, Z., Zhang, L., and Alexander, B., 2019. Heterogeneous sulfate aerosol formation mechanisms during wintertime Chinese haze events: air quality model assessment using observations of sulfate oxygen isotopes in Beijing, Atmos. Chem. Phys., 19, 6107–6123, https://doi.org/10.5194/acp-19-6107-2019.